Calculation of Radiation Dose at a Bone-to-Marrow Interface Using Monte Carlo Modeling Techniques (EGS4)

J. Christopher Johnson, Susan M. Langhorst, Sudarshan K. Loyalka, Wynn A. Volkert, and Alan R. Ketring

Army Materiel Command, Office of the Command Surgeon, Alexandria, Virginia; University of Missouri Research Reactor, Columbia, Missouri; Department of Nuclear Engineering, Columbia, Missouri; and Department of Nuclear Medicine, Veterans Hospital, Columbia, Missouri

Radiation dose rate profiles at a bone-to-marrow interface were calculated by simulating a uniform radiation source at the center of the endosteal layer in a long bone. Isotopes (^{153}Sm, ^{186}Re, and ^{166}Ho) were assumed to assimilate as surface agents and the dose profiles were calculated on a microscopic scale using the Electron-Gamma Shower (EGS4) computer program. We validated our computational model against published dose factors (δ) for uniform volume distributed sources replicating them to an accuracy of better than 95%. The calculated dose distributions illustrate the relative contribution of atomic electrons, beta, and photon fractions. The backscatter contribution to marrow dose increased from 3% to 4% at the source to 6% to 8% at a marrow depth of 100 μm. Backscattered dose fraction was not significantly different among the three isotopes. The dose contribution from the three isotopes was remarkably similar at ranges between 25 and 125 μm.

J Nucl Med 1992; 33:623–628

Samarium - 153 - ethylenediamineteramethylenephosophonic acid (^{153}Sm-EDTMP) has been successfully used to treat calcific cancers in dogs (*1*) and for palliation of pain from skeletal metastases in dogs (*2*) and humans (*2–4*). Localization of this chelate in bone marrow is minimal due to its rapid and efficient clearance from blood and soft tissue (*3–7*). Thus, radiation-induced marrow toxicity is primarily produced by irradiation of bone marrow by the relatively modest energy beta particles emitted from the ^{153}Sm-EDTMP deposited on the endosteal surfaces of bone (*8,9*). Radiation-induced reduction in circulating leukocytes and platelets in dogs is produced with escalating administered doses (i.e., incrementally increasing mCi ^{153}Sm-EDTMP/kg body weight) (*10*), but not at the rate predicted from whole-body external beam irradiations based on the MIRD methods for estimating the radiation dose to active marrow (*8,10*). In addition, Applebaum et al. (*8*) showed that increasing administered doses to extreme levels (i.e., up to 30 mCi ^{153}Sm-EDTMP/kg) did not result in complete marrow ablation. Marrow biospies in different regions of the skeleton of dogs showed that the marrow spaces surrounding trabecular bone became aplastic after receiving ≥ (6 mCi) ^{153}Sm-EDTMP/kg (*8*). The marrow space in the midshaft region of the femur, an area which normally supports little marrow function, showed some marrow activity after irradiation and exhibited abundant hematopoiesis 21 days after administration (*8*). These data indicate that some bone marrow cells in the medullary cavity do not receive radiation doses from the ^{153}Sm-EDTMP deposited on the endosteum due to the limited range of the ^{153}Sm-beta particles (*8*).

Studies with ^{166}Ho-EDTMP, a chelate with the same skeletal uptake and biodistribution properties as ^{153}Sm-EDTMP, showed it to be more effective in producing marrow suppression and bone marrow ablation (*11*). Holmium-166 emits a higher energy beta particle which makes more cells in the marrow cavity accessible to beta irradiation from bone absorbed ^{166}Ho. In order to better understand the influence of beta particle energy on marrow suppression or ablation properties, it is important to better understand the microdosimetry of radionuclides deposited on bone surfaces.

To characterize dosimetric properties of various beta-emitting isotopes proposed for use as surface-seeking radiotherapeutic agents, we developed a model based upon the Electron Gamma Shower (EGS4) computer code (*12, 13*). The advantage of this method is that one need not assume a homogeneous medium as required by most analytical methods. Thus, one can estimate the dose to tissues in the immediate vicinity of the cortical bone-to-marrow interface. The model is particularly useful because it provides a rapid and convenient method by which to compare dose distributions from radioisotopes having differing emission spectra prior to more complex and costly animal and clinical studies.

Received May 23, 1991; revision accepted Nov. 20, 1991.

For reprints contact: U.S. Army Materiel Command, ATTN: AMCSG-R (LTC Johnson), 5001 Eisenhower Ave., Alexandria, VA 22333.

Disclaimer: The work presented in this paper is solely that of the authors and in no way reflects the official policy or position of the U.S. Government or any agency thereof.

In this study, we have characterized the dose profiles for three isotopes: ^{166}Ho, ^{186}Re, and ^{153}Sm. These were chosen because they are of current interest as radiotherapeutic agents, and each emits different maximum beta energies ranging from relatively low (0.69 MeV for ^{153}Sm) to moderate (1.076 MeV for ^{186}Re) to high (1.855 MeV for ^{166}Ho) (*14*).

MATERIALS AND METHODS

Cortical Bone/Endosteum/Marrow Interface

Since the focus of this paper is on dosimetry of a very small area of bone marrow in the medullary cavity, we have used planar approximation of the interface between marrow and cortical bone (Fig. 1). It is typical of the inside wall of a long bone at the middle of the shaft (e.g., mid-femur). A planar model was a reasonable approximation because the area of particular interest on the inner surface of the bone was limited to a depth of a few hundred microns.

The endosteum, which lines the inside surface of the cavity, was modeled as a 10-μm thick slab between the marrow and the cortical bone. The cortical bone was assumed to be 0.225 cm thick. The backscatter contribution from tissue surrounding the cortical bone (muscle, ligaments, etc.) was neglected. Particle histories were terminated at the outer bone surface.

The radiation source was assumed to deposit at midplane in the endosteum. This source location approximates the deposition of radiotherapy drugs such as ^{153}Sm-EDTMP which deposit primarily on bone surfaces and have minimal deposition in the bone marrow (*8*).

Tissue Cross Sections

Radiological properties for the tissues under study were approximated by those of analog materials for which cross sections were available. Bone lining cells, endosteum and blood were represented by A150 tissue equivalent plastic since their radiological properties are similar. Cortical bone was represented by "ICRP cortical bone" (*15*). Cross-section tables were calculated from this data using the PEGS computer code (*12*).

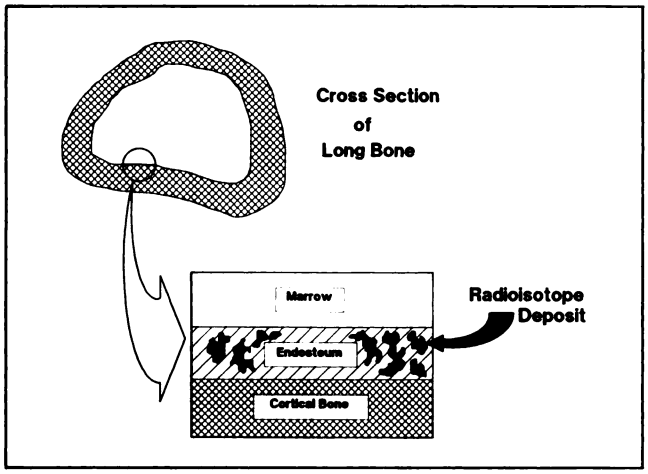

FIGURE 1. Planar representation of cortical bone-to-marrow interface in marrow cavity of long bones.

Isotope Spectra

The spectral characteristics for all three isotopes are well documented by Browne et al. (*16*) whose data we used for photon and atomic electron spectra. Hogan (*17*) provides more detailed beta spectra that we used for the beta portions of the dose calculations.

Planar Dose Regions

Twenty planar dose regions (slabs) were defined in this calculation to represent the region at the cortical bone to marrow interface. The outermost regions were thick compared to the range of the electrons in the isotope spectra. These end regions provided backscatter but were not used in calculating dose.

For each of the remaining inner slabs, the dose in the region is given by:

$$D_s = \Delta E \frac{\kappa}{\Delta T \rho N}, \qquad \text{Eq. 1}$$

where

- D_s is dose to the slab (Gy-cm^2/Bq-s).
- ΔE is energy deposited in the slab (MeV).
- κ is a unit conversion constant. $\left(\frac{1.602 \times 10^{-13} J}{MeV} \times \frac{1000\ g}{kg}\right)$
- ΔT is the thickness of the plate (cm).
- ρ is the density of the material (g/cm^3).
- N is the number of nuclear disintegrations of isotope deposited in the endosteal layer (Bq-sec).

Primary and Backscatter Contributions

We used this model to calculate two contributors to total soft-tissue dose: primary dose and backscattered dose. Primary dose arises from the energy deposited by the source when surrounded by a homogeneous medium. The backscattered dose is the additional energy deposited in the soft tissue due to radiation that is scattered back from the cortical bone layer into the soft tissue.

To calculate this backscatter dose, the simulation was run once as described above with the source at the boundary between the cortical and soft-tissue layers and again with the cortical bone replaced by soft tissue giving a homogeneous soft-tissue structure. Doses in corresponding regions from the all-tissue case were subtracted from those of the inhomogeneous case. The resulting backscatter dose was divided by the dose from the all-tissue simulation to get a percentage backscatter figure.

In summary:

$$B_i = \frac{D_{b,i} - D_{h,i}}{D_{h,i}} \times 100\%, \qquad \text{Eq. 2}$$

where

- B_i is the percent increase in dose to tissue due to backscattered radiation from the bone layer in the i^{th} dose region.
- $D_{b,i}$ is dose in the i^{th} dose region for the condition where the bone/marrow interface is present.
- $D_{h,i}$ is dose in the i^{th} dose region for the homogeneous, all-tissue condition, in the absence of the bone/marrow interface.

Backscatter was calculated for the composite spectrum as well as for individual components of the spectrum (beta, atomic electron, and photon).

Statistical Batch Processing

The initial incident particles were divided into 10 equal groups. Energy deposition for each group is accumulated separately. At the end of the simulation, the energy values for the ten groups were used to find a mean dose and associated standard deviation. For ease of interpretation, the error on the dose value is expressed in percent as a coefficient of variation, CV%:

$$CV\% = \frac{\bar{X}}{\sigma} \times 100\%, \qquad \text{Eq. 3}$$

where $CV\%$ is the coefficient of variation in percent; $\bar{X}$ is the sample mean, and σ is the sample standard deviation.

PRESTA

We used the Parameter Reduced Step Algorithm (PRESTA) (*18*) along with the EGS4 model in order to optimize performance of the model and reduce dependence on transport step size. The PRESTA parameters are given in Table 1.

Default values for PRESTA were used for all but the lateral crossing algorithm (LCA). The LCA correction is not required in this application where regions are only tens of microns thick and its use can create computational problems.

Hardware

All calculations for this paper were made using a VAX 8650 computer and VAX FORTRAN compiler. Nominal execution (CPU) times for total dose ranged from 15 to 40 min, while backscatter calculations took from 150 to 360 min to complete.

Validation of the Dose Model

To assure accuracy of the dosimetry model, we calculated dose deposition for a uniformly distributed source in an infinite homogeneous medium. Mean beta energy and beta dose constants were calculated for each of the three isotopes and compared to values published in the literature (*16,17,19*). The results of this validation are presented in Table 2 for mean beta energy and Table 3 for beta dose constants.

TABLE 1
Parameters for the PRESTA Algorithm

Parameter	Value used
Maximum energy loss step size (ESTEPE)	0.10
Electron cutoff energy	10 kev
Photon cutoff energy	1 kev
PRESTA parameters*:	
IPLC	0, (do path length correction)
IBCA	0, (use boundary crossing algorithm)
ILCA	1, (do *not* use lateral correction algorithm)
IOLDTM	0, (use new path length selection algorithm)
BLCMIN	0.0, (use default BLC algorithm)

* The importance of these parameters to the model output are described by Bielajew and Rogers (*18*).

TABLE 2
Comparison of Mean Beta Energies (keV), $\bar{E}_\beta$, Between Model and Published Values

	Investigator			
Isotope	This work	Hogan (*17*)	Browne (*16*)	Kocher (*19*)
^{166}Ho	617	610	711	665.7
^{186}Re	343	341	323	349.3
^{153}Sm	222	220	225	223.6

The values of mean beta energy, $\bar{E}_\beta$, for ^{186}Re and ^{153}Sm are very close to those given by other investigators (*16,17,19*). However, there is no general agreement on the value of mean beta energy for ^{166}Ho. Our results are nearest to those given by Hogan (*17*), on whose beta spectra we based the simulation.

The small differences between Kocher (*19*) and these calculations are attributable in part to the statistical error in the Monte Carlo simulation. That error is a function of the number of particles transported and was set a priori to ±5% over a 300-micron band surrounding the source.

RESULTS

The results of this work consist of depth-dose values for surface-seeking beta emitters deposited in the shaft of a typical long bone. They are presented graphically as radiation dose factors which lend themselves to clinical application (cGy-cm^2/μCi-hr). This is analogous to the volumetric "S" factor (cGy/μCi-hr) that has been used in MIRD calculations for ^{153}Sm (*9*). To determine the dose (cGy) to tissue at some distance from the source one multiplies the dose factor by the cumulated areal concentration (μCi-hr/cm^2) of the isotope on the surface. It is assumed that the isotope concentration is known, or can be determined, from autoradiography or by other means.

The Monte Carlo nature of the calculation causes the variance in the dose factors to increase with distance from the source as the magnitude of the deposited energy declines. At the source, the dose factors have a standard deviation of less than 1% of the mean. This increases to 4%–6% at a source to target distance of 300 μm. However,

TABLE 3
Validation Against Published Beta Dose Constant Data

	Beta Dose Constant, (Δ) (gm-cGy/μCi-hr)		
Isotope	This work	Kocher*	Difference (%)
^{166}Ho	1.431	1.420	+0.8
^{186}Re	0.692	0.692	+0.0
^{153}Sm	0.482	0.476	+1.3

* Because this model was based upon Hogan's spectral data (*17*), model output has been multiplied by the ratio of Kocher's stated $\bar{E}_\beta$ (*19*) to Hogan's $\bar{E}_\beta$. This was done in this comparison to compensate for the difference between the mean beta energies reported by the two authors.

if one considers the dose uncertainty as a fraction of peak (endosteal) dose, the error for depths to 300 μm is always less than 1%.

Figure 2 shows the calculated dose factors for all three isotopes for comparison over the entire region of ±2000 μm. Figure 3 shows the same data in the immediate vicinity of the source (±125 μm).

Dose Factors Versus Distance

From the data in Figure 2, one can see that the decrease in dose factor with distance has three distinct regions. The first region is marked by a precipitous decline within 50 μm of the source. This is primarily due to the rapid absorption of atomic electron emissions. The highest dose to the endosteum is delivered by the isotope with the lowest beta energy, ^{153}Sm, due to the abundance (absolute = 1.34) and relatively high energy (45 keV) of atomic electrons emitted from ^{153}Sm decay. The average range of these electrons is about 25 μm (20). Thus, they deposit most of their energy in the immediate vicinity of the source.

In the second region, beginning about 50 microns from the source, the atomic electron component ceases to be a factor and the deposited dose exponentially exhibits decreasing behavior dependent on the mean beta energy. It is important to note that the difference in dose constant between the three isotopes in the region 25–125 μm (Fig. 3) is slight despite their radically different spectral characteristics.

Regression of the linear portion of the semilogarithmic curves (on the marrow side) yields effective "dose factor attenuation coefficients" of: 10.6, 22.0, and 36.5 cm^{-1} for ^{166}Ho, ^{186}Re and ^{153}Sm, respectively. Corresponding intercept dose factor constants are 5.69, 6.06 and 6.48 cGy-cm^2/μCi-hr. The fit is good ($r^2 > 0.997$) for all isotopes. Regression of the dose attenuation constants for the three isotopes with respect to maximum beta energy results in an excellent fit ($r^2 = 0.995$) to a power function.

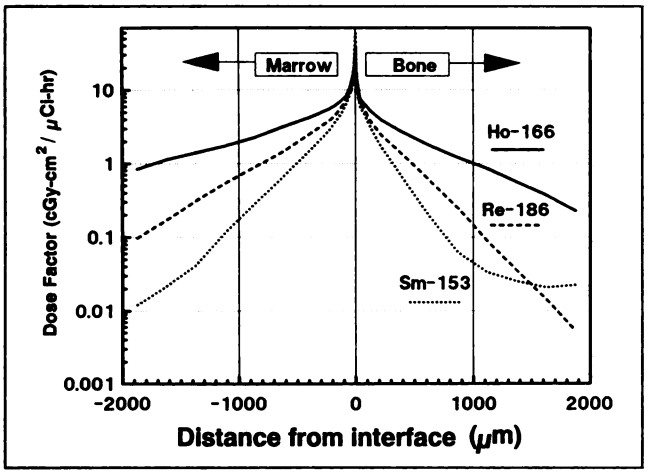

FIGURE 2. Dose rate factors (cGy-cm^2/μCi-hr) for ^{153}Sm, ^{186}Re and ^{166}Ho as a function of distance (0–2000 μm) from the cortical bone-to-marrow interface in long bones assuming uniform radionuclide deposition at midplane in the endosteum.

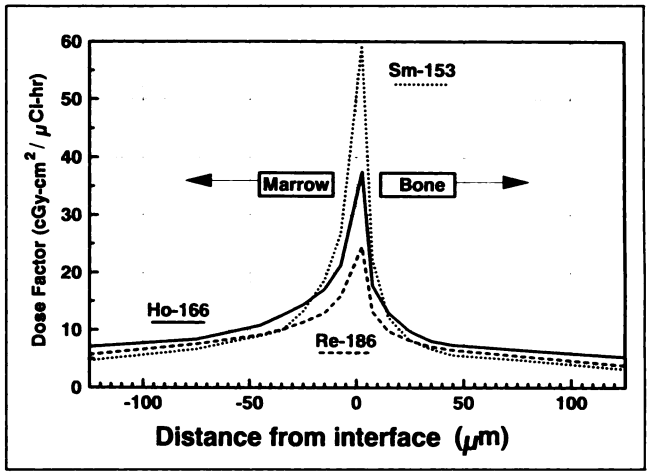

FIGURE 3. Dose rate factors (cGy-cm^2/μCi-hr) for ^{153}Sm, ^{186}Re and ^{166}Ho as a function of distance (0–125 μm) from the cortical bone-to-marrow interface in long bones assuming uniform radionuclide deposition at midplane in the endosteum.

Thus, the radiation dose factor in this predominantly beta region can be expressed in the form:

$$D = D_o e^{-\mu x}, \qquad \text{Eq. 4}$$

where

- D is the dose factor at depth x.
- D_o is the dose factor at the intercept.
- μ is the dose factor attenuation constant in cm^{-1} which can be expressed as:

$$\mu = 25.7\ E_{\beta max}{}^{-1.47}, \qquad \text{Eq. 5}$$

where $E_{\beta max}$ is the maximum beta energy for the isotope in MeV.

- x is the depth measured from the source in cm.

This exponential range of the betas extends from approximately 200 μm to 1300 μm for ^{153}Sm and beyond 2000 μm for ^{186}Re and ^{166}Ho. The relative magnitudes of radiation dose factors for the three isotopes in this region are as expected with ^{166}Ho resulting in the highest dose while ^{153}Sm delivers the lowest.

The third region of the radiation dose factor curves is seen primarily on the bone side of the graph for ^{153}Sm (Fig. 2). At about 1300 μm into the bone, the dose factor for ^{153}Sm begins to flatten out while that of ^{186}Re and ^{166}Ho continue in steep decline. This is due to the total depletion of ^{153}Sm betas which occurs at their maximum range (about 1700 μm). Beyond this, the photon component of ^{153}Sm is the primary contributor to dose which results in the flattening of the dose factor curve. For ^{166}Ho and ^{186}Re, the beta range is greater than the range plotted so that the photon plateau is not yet seen.

Backscatter

The concept of backscatter is useful in illustrating the effect of cortical bone on dose to adjacent soft tissue. Backscatter is radiation scattered by cortical bone back into the soft tissue where it originated. We found that the backscatter contribution to soft-tissue dose adjacent to the bone/marrow interface was approximately 4% at the interface, building up to about 7%–8% at 100 μm from the interface (Fig. 4).

The statistical error in the backscatter calculation was similar and substantial for all of the three isotopes and the backscatter fractions for the three isotopes were not statistically different from each other. The backscatter due to ^{153}Sm dissipates most rapidly with range because of the low energy of the ^{153}Sm betas. Variance in ^{153}Sm dose factor curve reaches 30% of the mean at about 200 μm, for ^{186}Re at about 300 μm and for ^{166}Ho, with the highest beta energy, at nearly 400 μm.

There was no discernible difference between the composite spectrum and beta-only spectrum, which indicated that the beta component of the atomic emissions was the primary contributor to backscatter dose. This was true for all three isotopes.

Near the source, the atomic electron contribution to backscatter was about the same as that from the beta segment, about 3%. As one would expect from the low energies of this spectrum, the backscatter was limited to the first two dose regions, i.e., 50 μm from the source. The results are shown in Table 4.

No significant backscatter contribution was found for photons. After running 350,000 photons, the standard deviation for the backscatter fraction was still on the order of 10 times the mean. These data should not be construed to mean that gamma backscatter does not occur, but rather that its magnitude does not contribute significantly to dose.

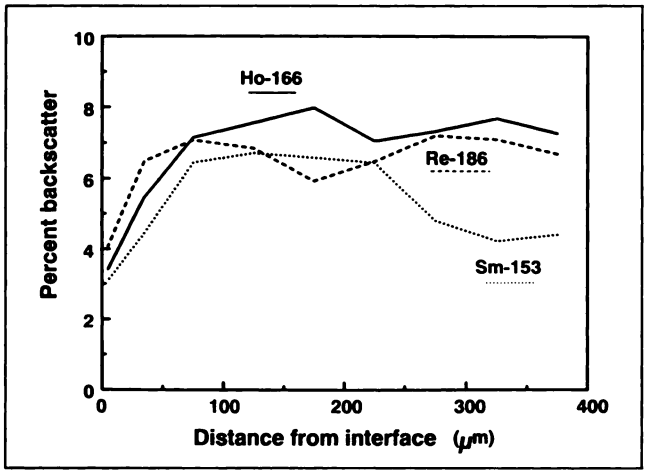

FIGURE 4. Comparison of the percent of total dose to bone marrow which is due to backscatter of the emissions from ^{166}Ho, ^{186}Re, and ^{153}Sm as a function of distance from the midplane of the endosteum.

TABLE 4
Backscatter from Atomic Electrons (%)

	Dose Region			
	0–10 μm		10–50 μm	
Isotope	$\bar{X}$*	σ†	$\bar{X}$*	σ†
^{166}Ho	2.85	0.82	2.28	1.48
^{186}Re	3.24	0.75	4.96	1.74
^{153}Sm	1.96	0.64	2.24	1.80
All three isotopes	2.68	1.28	3.16	2.90

* Mean percent backscatter in stated region.
† Standard deviation of percent backscatter in stated region.

CONCLUSIONS

Calculation of radiation dosimetry to the bone marrow from radionuclides deposited on bone surfaces is a difficult problem due to the complex geometry of the soft-tissue and bone intermixture (*21–24*). Treatment of this problem has been hampered by difficulties in modeling the intricate microscopic intermixture of soft tissue and bone (*21,24*). The radiosensitive hematopoietic cells reside primarily within the marrow space of trabecular bone (*22*), with some also found in the medullary cavity long bones. Models and methods of calculating the energy deposition from beta-emitters deposited on trabecular surface have been developed to calculate marrow doses in these cavities (*21,22,24*). The size of these cavities are small and often the range of the beta particles are sufficiently long that they will traverse several cavities while depositing energy along their tracks (*21*). As a result, the radiation dose delivered from skeletal-seeking beta-emitting radiopharmaceuticals is more homogeneous to marrow in trabecular bone than marrow in the larger medullary cavities of long bone. At higher radiation doses, the marrow in trabecular bone will be severely depleted (*8*) and the resulting maximal depression of circulating leukocyte and platelet counts in the blood stream will be primarily dependent upon the microdosimetry to marrow cells in long bones (*8,10*). The results of this study illustrate the high degree of inhomogeneity in the radiation dose profile for this marrow in the long bones. The results also demonstrate the large differences that exist between dose rate constants for ^{166}Ho relative to less energetic ^{153}Sm at distances from the bone surface of ≥150 μm (Fig. 2).

Radiation dose profiles (expressed as dose rate constants) were computed for tissue at and adjacent to a bone marrow interface on the medullary cavity. A Monte Carlo method, based upon the EGS4 computer code, was used for the calculation to account for the inhomogeneity at the transition from marrow to cortical bone. Backscattered radiation from the cortical bone contributed 3%–4% to the dose at the interface (in the endosteum). The percentage of backscatter increased to 6%–8% at a distance of 100 μm into the marrow and remained approximately constant (Fig. 4).

Although ^{153}Sm, ^{186}Re, and ^{166}Ho spanned a rather wide range of maximum beta energies, the calculated dose constants were within a few percent (±20%) in the range of 25–125 μm from the surface (Fig. 3). In the endosteum, however, the dose factors from these radionuclides are significantly different, with ^{153}Sm and ^{186}Re producing the highest and lowest dose rate factor, respectively (Fig. 3). These differences in dose rate factors at and near the interface reflect the relative abundances of atomic electrons in the isotope emission spectra of the respective radionuclides. Beyond distances of 125–150 μm, beta-particles were the predominant factor in determining the dose rate factors (Fig. 2).

Calculation of the radiation dose rate factor profiles in marrow cavities of long bones for radionuclides with different energy beta-particle emissions makes it possible to relate the maximal degree of myelosuppressive activity with the radiation dose to sensitive hematopoietic cells residing >150 μm from the endosteal surface. This work shows that the EGS4 method is a valuable tool for dose estimation in intentional marrow ablation [e.g., marrow transplant preparative regimes (*11*)] or in treatment of primary or metastatic bone cancers for which maximal sparing of marrow cells at therapeutically efficacious doses is desirable (*2,6,4,7*).

ACKNOWLEDGMENTS

The principal author gratefully acknowledges the U.S. Army Medical Department for their support of this work. We are all grateful to Dr. Julie Dawson, Mr. Lynn Diel and the staff of the University of Missouri Engineering Computer Network for their assistance in providing computer resources.

REFERENCES

1. Howell RW, Rao DV, Sastry KS. Macroscopic dosimetry for radioimmunotherapy: nonuniform activity distributions in solid tumors. *Med Phys* 1989;16:66–74.
2. Holmes RA, Farhangi M. Dose tolerance of ^{153}Sm-EDTMP in metastatic bone cancer. *J Nucl Med* 1988;29:775.
3. Singh A, Holmes RA, Farhangi M, et al. Human pharmacokinetic of ^{153}Sm-EDTMP in metastatic cancer. *J Nucl Med* 1989;30:1814–1818.
4. Turner HJ, Caringbold PG, Hetherington EL, Sorby P, Martindale AA. A phase I study of ^{153}Sm-EDTMP therapy for disseminated skeletal metastases. *J Clin Oncol* 1989;7:1926–1931.
5. Goeckeler WF, Edwards B, Volkert WA, et al. Skeletal localization of ^{153}Sm chelates: potential therapeutic bone agents. *J Nucl Med* 1987;28:495–504.
6. Ketring AR. ^{153}Sm-EDTMP and ^{186}Re-HEDP as bone therapeutic radiopharmaceuticals. *Nucl Med Biol* 1987;14:223–232.
7. Volkert WA, Simon J, Ketring AR, Holmes RA, Lattimer JC, Corwin, LA. Radiolabeled phosphonic acid chelates: potential therapeutic agents for treatment of skeletal metastases. *Drugs of Future* 1989;14:799–811.
8. Appelbaum FR, Sandmaier B, Brown P, et al. Myelosuppression and mechanism of recovery following administration of ^{153}Sm-EDTMP. *Antibody, Immunoconj and Radiopharm* 1988;1:263.
9. Logan KW, Volkert WA, Holmes RA. Radiation dose calculations in persons receiving injection of ^{153}Sm-EDTMP. *J Nucl Med* 1987;28:505–509.
10. Lattimer JC, Corwin LA, Stapleton J, et al. Clinical clinicopathologic effects of samarium-153-EDTMP administered intravenously in normal dogs. *J Nucl Med* 1990;31:586–593.
11. Appelbaum FR, Brown P, Sandmaier B, et al. Development of improved marrow transplant preparative regimens. II. Use of aminophosphonic acid-radionuclide conjugates. Tech Proc ACNP-SNM Joint Symp on Bio-Radionuclide Therapy, 1988.
12. Nelson WR, Hirayama H, Rogers DWO. The EGS4 code system. Stanford, CA: Stanford Linear Accelerator Center; Report No. SLAC-265; 1985.
13. Rogers DWO. Low energy electron transport with EGS. *Nucl Instrum Meth* 1984;227:535.
14. Walker FW, Miller DG, Feiner F. *Nuclides & isotopes*, thirteenth edition. Schenectady, NY: General Electric Co., Knolls Atomic Power Laboratory; 1983.
15. International Commission on Radiological Protection. *Report of the task group on reference man.* Oxford: Pergamon Press; ICRP Publication 23; 1975.
16. Browne E, Firestone RB, Shirley VS. *Table of radioactive isotopes.* New York: John Wiley & Sons; 1986.
17. Hogan OH, Zigman PE, Mackin JL. *Beta spectra II: spectra of individual negatron emitters.* San Francisco, CA: US Navy Radiological Defense Laboratory; Report No. USNRDL-TR-802; 1964.
18. Bielajew AF, Rogers DWO. PRESTA: the parameter reduced electron-step transport algorithm for electron Monte Carlo transport. *Nucl Instrum Meth Phys Res* 1987;B18:165–181.
19. Kocher DC. *Radioactivity decay tables.* Springfield, VA: NTIS; Report No. DOE/TIC-11026, 1981.
20. U.S. Department of Health, Education and Welfare. *Radiological health handbook.* Rockville, MD: Bureau of Radiological Health; 1970:29,123.
21. Eckerman KF. Aspects of the dosimetry of radionuclides within the skeleton with particular emphasis on the active marrow. In: *Fourth international radiopharmaceutical dosimetry symposium proceedings* [CONF-851113—(DE86010102)]. Springfield, VA: NTIS; 1985:514–534.
22. ICRP Publication 30. *Limits for intakes of radionuclides by workers.* Oxford, UK: Pergamon Press; 1979.
23. Beddoe AH, Darby PJ, Spiers FW. Measurements of trabecular bone structure in man. *Phys Med Biol* 1976;21:589–607.
24. Spiers FW, Whitwell JR, Beddoe AH. Calculated dose factors for radiosensitive tissues in bone irradiated by surface-deposited radionuclides. *Phys Med Biol* 1978;23:484–494.